Biogeosciences Discuss., 10, 5175–5221, 2013
www.biogeosciences-discuss.net/10/5175/2013/
doi:10.5194/bgd-10-5175-2013

Biogeosciences
Discussions
Open Access

Dynamics of dissolved inorganic carbon and aquatic metabolism in the Tana River Basin, Kenya

F. Tamooh[1,2], A. V. Borges[5], F. J. R. Meysman[3,4], K. Van Den Meersche[3,*], F. Dehairs[3], R. Merckx[1], and S. Bouillon[1]

[1]Katholieke Universiteit Leuven, Department of Earth and Environmental Sciences, Celestijnenlaan 200E, 3001 Leuven, Belgium
[2]Kenya Wildlife Service, P.O. Box 82144-80100, Mombasa, Kenya
[3]Vrije Universiteit Brussel, Department of Analytical and Environmental Chemistry, Pleinlaan 2, 1050 Brussel, Belgium
[4]Royal Netherlands Institute of Sea Research, Korringaweg 7, 4401 NT Yerseke, the Netherlands
[5]Université de Liège, Unité d'Océanographie Chimique, Allée du 6 Août, 17, 4000, Belgium
[*]now at: French Agricultural Research Centre for International Development, UMR Eco&Sols, SUP AGRO Bât 12, 2 Place Viala, 34060 Montpellier Cedex 2, France

Received: 28 February 2013 – Accepted: 5 March 2013 – Published: 14 March 2013

Correspondence to: F. Tamooh (fredrick.tamooh@ees.kuleuven.be) and S. Bouillon (steven.bouillon@ees.kuleuven.be)

Published by Copernicus Publications on behalf of the European Geosciences Union.

Abstract

A basin-wide study was conducted in the Tana River Basin (Kenya), in February 2008 (dry season), September–November 2009 (wet season), and June–July 2010 (end of the wet season) to assess the dynamics and sources of dissolved inorganic carbon (DIC) as well as to quantify CO_2 fluxes, community respiration (R), and primary production (P). Samples were collected along the altitudinal gradient (from 3600 m to 8 m) in several headwater streams, reservoirs (Kamburu and Masinga), and main Tana River. DIC concentrations ranged from 0.2 mmol L^{-1} to 4.8 mmol L^{-1} but with exceptionally high values (3.5 ± 1.6 mmol L^{-1}) in Nyambene Hills tributaries. The wide range of $\delta^{13}C_{DIC}$ values (−15.0 ‰ to −2.4 ‰) indicate variable sources of DIC with headwater streams recording higher signatures compared to main Tana River. With few exceptions, the entire riverine network was supersaturated in CO_2, implying the system is a net source of CO_2 to the atmosphere. pCO_2 values were generally higher in the lower main Tana River compared to headwater tributaries, opposite to the pattern typically observed in other river networks. This was attributed to high suspended sediment in the main Tana River fuelling in-stream community respiration and net heterotrophy. This was particularly evident during 2009 wet season campaign (median pCO_2 of 1432 ppm) compared to 2010 end of wet season (1002 ppm) and 2008 dry season (579 ppm). First-order estimates show in-stream community respiration was responsible for the bulk of total CO_2 evasion (59 % to 89 %) in main Tana River while in tributaries respiration accounted for 4 % to 52 % of total CO_2 evasion, suggesting CO_2 evasion in tributaries was sustained by processes than respiration, such as CO_2-oversaturated groundwater input. While sediment loads increase downstream and thus light availability decreases in the water column, both chlorophyll a (0.2 µg L^{-1} to 9.6 µg L^{-1}) and primary production (0.004 µmol L^{-1} h^{-1} to 7.38 µmol L^{-1} h^{-1}) increased consistently downstream. Diurnal fluctuations of biogeochemical processes were examined at three different sites along the river continuum (headwater, reservoir, and mainstream), and were found to be substantial only in the headwater stream, moderate in the reservoir and not detectable at main Tana River. The pronounced diurnal fluctuations observed in the headwater stream were largely regulated by periphyton as deduced from the low chlorophyll a in the water column.

1 Introduction

Rivers are increasingly recognized as important not only in the transport of carbon (C) between the terrestrial and marine environments, but also in terms of C storage and processing. River systems are typically a source of CO_2 to the atmosphere partly due to receiving CO_2-rich groundwater and partly due to heterotrophic processes within the system. Thus, dissolved inorganic carbon (DIC, comprising both HCO_3^-, CO_3^{2-} and CO_2) is an important component in river biogeochemistry. The dynamics of riverine DIC are primarily controlled by watershed inputs and in-stream processes, which lead to either addition or removal of carbon from the DIC pool and which also change the $\delta^{13}C_{DIC}$ values of riverine water (Fig. 1). The input of terrestrial organic matter (and the relative contribution of C3 over C4 plants to this), the weathering of carbonate/silicate minerals within the bedrock, and the ratio of groundwater discharge to surface runoff are the major watershed processes controlling the dynamics of riverine DIC and its $\delta^{13}C$ signature. Further, CO_2 exchange with atmosphere, in stream dissolution or precipitation of carbonate/silicate minerals, primary production (P) and community respiration (R) are the additional in-stream processes impacting DIC dynamics (McConnaughey et al., 1994; Amiotte-Suchet et al., 1999; Abril et al., 2003; Finlay and Kendall, 2007). The strength of each of these processes depends on the size of the river, its productivity (Finlay, 2003) as well as the geology and hydrology of the basin (Bullen and Kendall, 1998), and varies seasonally as a function of temperature and discharge. The complexity of all these processes and their interplay makes it difficult to constrain the sources of riverine DIC.

Riverine carbon undergoes a high degree of transformation and some degree of retention as it cycles from the terrestrial biosphere to the ocean (Cole et al., 2007;

Aufdenkampe et al., 2011). In most cases, this results in supersaturation of CO_2 in fluvial systems and significant CO_2 evasion to the atmosphere (Kempe, 1984; Telmer and Veizer, 1999; Cole and Caraco, 2001; Richey et al., 2002; Cole et al., 2007; Aufdenkampe et al., 2011). Quantitative assessment of riverine CO_2 degassing in tropical rivers is critical in the perspective of carbon cycling, particularly considering that tropical systems account for ∼ 70 % of global riverine carbon fluxes partly owing to their large areal extent, varying climatic conditions and diverse land-use covers (Milliman and Farnsworth, 2011).

The global freshwater systems CO_2 evasion to the atmosphere is estimated to be in the order of $\sim 3.3\,Pg\,C\,yr^{-1}$, three-fold greater than total carbon transport ($\sim 0.9\,Pg\,C\,yr^{-1}$) to the global ocean (Aufdenkampe et al., 2011; Butman and Raymond, 2011). Such high CO_2 evasion necessitates improved understanding of DIC dynamics in both local and regional systems and underlying drivers of carbon cycling. While the above CO_2 evasion estimate is prone to large uncertainty, a range of estimates have been proposed, with Cole et al. (2007) giving a much more conservative number of $0.75\,Pg\,C\,yr^{-1}$. This is partly due to lack of sufficient data to provide a representative and correct scaled flux, particularly in tropical systems.

In recent years, the application of isotopic proxies has become invaluable in understanding riverine carbon cycling. Based on the premise that various carbon sources have distinct $\delta^{13}C$ values, $\delta^{13}C_{DIC}$ signatures have been used in a wide range of fluvial systems to constrain the biological and geological sources of DIC (Amiotte-Suchet et al., 1999; Finlay, 2003; Doctor et al., 2008; Brunet et al., 2005, 2009). For instance, riverine DIC predominantly derived from oxidation of organic matter will have $\delta^{13}C$ values (about −28 ‰ and −13 ‰ for by C3 and C4 plants respectively), −8 ‰ if derived from atmospheric air exchange, whereas $CaCO_3$ dissolution will shift $\delta^{13}C$ value to heavier values ($\delta^{13}C$ value carbonate is close to 0 ‰ if from marine origin) (Finlay, 2003; Brunet et al., 2005, 2009). Despite the fact that different sources have distinct isotopic values, the interpretation of variations in $\delta^{13}C_{DIC}$ remains a challenge, since

processes such as in-stream respiration and primary production, and isotopic equilibration with atmospheric CO_2 cause fractionation (Amiotte-Suchet et al., 1999).

According to the River Continuum Concept (RCC, Vannote et al., 1980), rivers show a predictable downstream variation in the linkage with the terrestrial environment. Thus, forested headwater streams (1st–3rd order) would be predominantly heterotrophic since metabolism is fuelled by allochthonous subsidies whereas, mid-order (4th–6th) streams would be predominantly autotrophic without significant riparian canopy cover. Large rivers (> 7th-order), revert to heterotrophy since P would be limited by increased turbidity and depth, thus R exceeds P. Quantitative estimation of riverine P and R rates are rarely assessed at basin-wide scale despite their significance in understanding the functioning of riverine systems yet most large rivers do not conform with the original tenets of RCC due to altered lateral exchange with floodplains and flow discontinuities (Maiolini and Bruno, 2007). Since the RCC, a variety of alternate concepts to describe matter and energy flow have been developed as reviewed by Bouwman et al. (2013). The metabolic balance between riverine P and R defines whether an ecosystem is net heterotrophic ($P : R < 1$) or net autotrophic ($P : R > 1$) (Odum, 1956; Venkiteswaran et al., 2007). Most heterotrophic freshwater aquatic systems are sustained by subsidies of organic materials input from terrestrial biome (Cole and Caraco, 2001), which decompose within the riverine system, and as such influence carbon concentrations and their isotopic composition. The predominant metabolic activity thus depends on the magnitude of allochthonous inputs and the subsequent fraction respired versus autochthonous production (Cole and Caraco, 2001).

With this background, the present study examines the riverine DIC dynamics and $\delta^{13}C_{DIC}$ isotopic values in the Tana River basin (Kenya), based on three basin wide sampling campaigns covering dry season, wet season, and end of wet season in order to constrain main sources of DIC. To quantify the strength of the riverine CO_2 sources, we estimated both pCO_2 and CO_2 fluxes in an attempt to identify the primary CO_2 evasion hotspots within Tana River basin. In addition, the study also examines the longitudinal changes in the magnitude of riverine P and R rates. We further examined

to what extent pelagic respiration sustained the CO_2 evasion. Finally, we monitored biogeochemical parameters during diurnal cycles at three different sites along the river continuum representing headwater streams, reservoirs and main Tana River.

2 Materials and methods

2.1 Study area

The Tana River is the longest river in Kenya (~ 1100 km), with a total catchment area of ~ 96 000 km^2 (Fig. 2a). The river system can be separated into two main parts, here referred to as "Tana headwaters" and the "lower main Tana". The Tana headwaters consists of numerous tributaries, which originate from the Aberdare Range in the central highlands of Kenya, the highlands around Mount Kenya, and the Nyambene Hills in eastern Kenya (Fig. 2a). The lower main Tana encompasses the section downstream of the Nyambene Hills, where the river flows southeast for about 700 km through semiarid plains. Along this stretch, tributaries only discharge in short pulses during the wet season. As a result, the lower main Tana forms a single transport channel during the dry season, delivering material to the Indian Ocean (Maingi and Marsh, 2002). The lower Tana River has extensive floodplains between the towns of Garissa and Garsen, but floodplain inundation was irregular in recent decades due to the river flow regulation by five hydroelectric dams upstream (Maingi and Marsh, 2002). The associated reservoirs have a combined surface area of ~ 150 km^2, and a significant amount of sediment is trapped by these dams (Dunne and Ongweny, 1976; Brown and Schneider, 1998). Masinga is the largest reservoir (commissioned in 1981) and has a surface area of ~ 113 km^2 and a storage capacity of ~ 1560×10^6 m^3, while the Kamburu reservoir (the second largest, commissioned in 1975) has a surface area ~ 15 km^2 and a storage capacity of ~ 147×10^6 m^3 (GOK-TARDA, 1982). The Tana River basin includes different ecological zones experiencing different rainfall patterns, decreasing from the headwaters (altitude> 3050 m, annual precipitation ~ 1800 mm yr^{-1}), upper highlands

(altitude 2450–3050 m, annual precipitation ~ 2200 mm yr^{-1}), midaltitude catchment (altitude 1850–900 m, annual precipitation between 900 and 1800 mm yr^{-1}), to the lower semiarid Tana catchment (altitude 900–10 m, annual precipitation between 450 and 900 mm yr^{-1}) (Brown and Schneider, 1998; Fig. 2b). The basin experiences a bimodal hydrological cycle, with long rains between March and May, and short rains between October and December, which also leads to a clear bimodal pattern in the river discharge (Fig. 3). The mean annual river discharge at the Garissa gauging station is 156 $m^3 s^{-1}$ over the period 1934 to 1975 (daily data from the Global River Discharge Database, available at: http://daac.ornl.gov/RIVDIS/rivdis.shtml). The high-altitude headwaters (Aberdare Range, Mt. Kenya) are characterized by mountainous forest vegetation and moorlands at the highest elevations, giving way to more intense agricultural activities in mid altitude regions. The semi-arid lower Tana is dominated by open to wooded savannah grassland, with some riverine gallery forests along the Tana River.

2.2 Sampling and analytical techniques

Sampling was carried out during three campaigns in February 2008 (dry season), September–November 2009 (wet season), and June–July 2010 (end of wet season) (Fig. 3). The average river discharge measured at Garissa station during the wet season (209 $m^3 s^{-1}$) was 1.7 higher than during the dry season (123 $m^3 s^{-1}$) and 1.4 times that of the end-of-wet-season (145 $m^3 s^{-1}$) (Fig. 3). Samples were taken throughout the river basin (Fig. 2a; Supplement Table 1); sampling sites included a subset of small streams in the headwater regions, an approximately equidistant set of locations along the main lower Tana River, and two of the five hydro-electric reservoirs (Masinga and Kamburu). The dry season campaign in February 2008 only covered a subset of these field sites; these data have already been presented in Bouillon et al. (2009), and are used here for comparison purposes. In both the 2009 and 2010 campaigns, an extensive basin-wide survey was carried out. In addition, three sampling sites (Chania

stream in Aberdare Range, Masinga reservoir and Tana River-Bura) were selected for a 24 h cycle sampling (Fig. 2a).

During the dry season and the wet season campaigns, water temperature and DO were measured in situ with polarographic electrode (WTW Oxi-340) calibrated on saturated air, with an accuracy of 0.1 % while pH was measured using a combined potentiometric electrode (Metrohm Thermo Orion model 230). A YSI ProPlus multimeter was used during end of wet season campaign. The pH probe was calibrated using United States National Bureau of Standards buffer solutions (4 and 7), respectively. The specific conductivity was normalized in the laboratory at 25 °C. Water samples for the analysis of $\delta^{13}C_{DIC}$ and $\delta^{18}O_{DO}$ were taken with a Niskin bottle at ~ 0.5 m below the water surface by gently overfilling 12 mL glass headspace vials, and poisoned with 20 µL of a saturated $HgCl_2$ solution. For the analysis of $\delta^{13}C_{DIC}$, a 2 mL helium (He) headspace was created, and H_3PO_4 was added to convert all DIC species to CO_2. After overnight equilibration, part of the headspace was injected in the stream of an elemental analyser–isotope ratio mass spectrometer (EA-IRMS; ThermoFinnigan Flash HT and ThermoFinnigan DeltaV Advantage) for $\delta^{13}C$ measurements. The obtained $\delta^{13}C$ data were corrected for the isotopic equilibration between gaseous and dissolved CO_2 as described in Gillikin and Bouillon (2007). Measurements were calibrated with certified reference materials LSVEC and either NBS-19 or IAEA-CO-1. For $\delta^{18}O_{DO}$, a similar headspace was created, after which samples were left to equilibrate for 2 h. $\delta^{18}O_{DO}$ was then measured using the same EA-IRMS setup by monitoring m/z 32, 33, and 34 and using a molecular sieve (5 Å) column to separate N_2 from O_2. Outside air was used as the internal standard to correct all $\delta^{18}O$ data.

Water samples for Total Alkalinity (TA) were obtained by prefiltering surface water through pre-combusted GF/F filters (0.7 µm), with further filtration through 0.2 µm syringe filters in high-density polyethylene bottles. TA was analyzed by automated electro-titration on 50 mL samples with 0.1 mol L^{-1} HCl as titrant (reproducibility estimated as better than ± 3 µmol kg^{-1} based on replicate analyses). The partial pressure of CO_2 (pCO_2) and DIC concentrations were computed from pH and TA measurements

using the carbonic acid dissociation constants for freshwater from Millero et al. (1979). The accuracy of computed DIC and pCO_2 values are estimated at ± 5 µmol L^{-1} and ± 5 ppm, respectively. Water samples for major elements (Ca^{2+} and Mg^{2+}) and nutrient (NO_3^-) were obtained in 20 mL scintillation vials the same way as TA samples, but were preserved with 20 µL of ultra-pure HNO_3 and 20 µL of a saturated $HgCl_2$ solution for major elements and nutrient, respectively. The concentrations of major elements were measured using Inductively Coupled Plasma-Atomic Emission Spectroscopy (Iris Advantage, Thermo Jarrel-Ash) while nutrients were measured using standard chromatographic techniques (ICS-900, Dionex).

Water-air CO_2 fluxes were measured using a custom-made floating chamber with a surface area and volume of approximately 0.045 m^2 and 5.2 L respectively, coupled with an infra-red CO_2 analyzer (Licor-820) and data logger. The floating chamber was placed on the surface of the water stationary for ~ 10 min. The slope of the linear regression between pCO_2 and time was obtained and used to calculate the CO_2 flux per unit area and per unit time.

Samples for phytoplankton pigment analysis were obtained by filtering a known volume of surface water on pre-combusted 47 mm GF/F filters, which were immediately packed in cryotubes and stored in liquid N_2. Upon return to the laboratory, the samples were stored at −20 °C until further analysis. Pigments were extracted in 10 mL of an acetone : water mixture (90 : 10), and a subsample was separated by high performance liquid chromatography on a C18 reverse phase column (Bouillon et al., 2009). Calibration was performed with working standards prepared from commercially available pure compounds.

The R rates were determined by quantifying the decrease in DO (using the polarographic electrode WTW Oxi-340) of river water incubated in dark cool box filled with water to retain ambient temperature for approximately 24 h using 250 mL bottles (2–3 replicates) with air-tight polycone caps. The P rates were quantified by determining the uptake of DIC after short-term (1–3 h) incubations of river water using 1 L polycarbonate bottle spiked with ^{13}C-labeled sodium bicarbonate ($NaH^{13}CO_3$). A sub-sample for

$\delta^{13}C_{DIC}$ of the spiked water was sampled for the purpose of computations. Samples for analysis of particulate organic carbon (POC) and $\delta^{13}C_{POC}$ were obtained at the start (natural abundance values) and at the end of the incubation by filtering a known volume of surface water on pre-combusted (overnight at 450 °C) 25 mm GF/F filters (0.7 µm). Filters were decarbonated with HCl fumes for 4 h, re-dried and packed into Ag cups. POC and $\delta^{13}C_{POC}$ were determined on a Thermo elemental analyser – isotope ratio mass spectrometer (EA-IRMS) system (FlashHT with DeltaV Advantage), using the TCD signal of the EA to quantify POC and by monitoring m/z 44, 45, and 46 on the IRMS. Quantification and calibration of $\delta^{13}C$ data was performed with IAEA-C6 and acetanilide that was calibrated against international standards. Reproducibility of $\delta^{13}C_{POC}$ measurements was typically better than 0.2 ‰. The P data here refers only to surface water (~ 0.5 m deep) measurements (not depth integrated). Calculations to quantify the rates were done as described in Dauchez et al. (1995).

3 Results

3.1 In situ measurements, dissolved inorganic carbon and $\delta^{13}C_{DIC}$

Generally, pH, temperature, and specific conductivity increased consistently downstream (Pearson correlation, $r^2 = 0.90$, 0.41 and 0.47 for temperature, pH and specific conductivity respectively, $p < 0.05$, $n = 132$) with water temperature ranging from 10.6 °C to 32.1 °C, pH from 6.61 to 8.71, specific conductivity from 11 µS cm^{-1} to 582 µS cm^{-1}, and DO from 41 % to 134 % during the 2008 dry season, 2009 wet season and 2010 end of wet season campaigns (Supplement Table 1; Supplement Figs. 1 and 2). DIC concentrations ranged from 0.2 mmol L^{-1} to 4.8 mmol L^{-1} with an overall mean of 1.1 ± 1.0 mmol L^{-1}. Exceptionally high values (3.5 ± 1.6 mmol L^{-1}) were systematically recorded in Nyambene Hills tributaries during all three campaigns (Fig. 4). DIC concentrations increased consistently downstream (Pearson correlation, $p < 0.01$, $r^2 = 0.67$, $n = 108$) when excluding values from Nyambene Hills tributaries. The DIC

concentrations within different tributaries were similar (paired t-test, $p > 0.05$) during the three campaigns. In contrast, Tana River mainstream DIC values were significantly higher (ANOVA, $p < 0.05$) during 2009 wet season campaign (1.3 ± 0.2 mmol L^{-1}) and lowest during 2010 end of wet season campaign (1.1 ± 0.2 mmol L^{-1}). TA showed a strong positive correlation with the sum of Ca^{2+} and Mg^{2+} concentration during all three campaigns (Pearson correlation, $p < 0.01$, $r^2 = 0.92$; $n = 125$; Fig. 5a).

$\delta^{13}C_{DIC}$ signatures ranged from −15.0 ‰ to −2.4 ‰ during the three campaigns. $\delta^{13}C_{DIC}$ values within different tributaries were similar (paired t-test, $p > 0.05$) during all the three campaigns, but Tana River mainstream recorded relatively depleted values (−11.2 ± 1.8 ‰) during 2009 wet season campaign compared to 2008 dry season and 2010 end of wet season campaigns combined (−8.7 ± 0.7 ‰). Overall, $\delta^{13}C_{DIC}$ showed a negative correlation with DIC concentrations (Pearson correlation, $p < 0.01$, $r^2 = 0.49$, $n = 122$) during all the three campaigns with tributaries from Aberdare and Mt. Kenya regions recording the lowest DIC concentrations (0.6 ± 0.3 mmol L^{-1}) and highest $\delta^{13}C_{DIC}$ signatures (−6.9 ± 2.7 ‰), Tana River mainstream intermediate DIC concentrations (1.2 ± 0.2 mmol L^{-1}) and $\delta^{13}C_{DIC}$ signatures (−9.7 ± 1.7 ‰), whereas Nyambene Hills tributaries recorded the highest DIC concentrations (3.5 ± 1.6 mmol L^{-1}) and the lowest $\delta^{13}C_{DIC}$ signatures (−11.3 ± 2.4 ‰). Unusually high $\delta^{13}C_{DIC}$ values were observed at Masinga reservoir (−4.5 ± 0.1 ‰) during the dry season, but this decreased rapidly to −8.9 ‰ less than 5 km downstream.

3.2 Dynamics of riverine pCO_2 and CO_2 fluxes

The whole river network with few exceptions was supersaturated with CO_2 (pCO_2 values between 110 and 5204 ppm) with respect to atmospheric equilibrium (385 ppm), with an overall median of 1002 ppm. Higher values were recorded during 2009 wet season campaign (median 1432 ppm) compared to 2010 end of the wet season (median 1002 ppm), whereas 2008 dry season was two-fold lower (median 579 ppm; Fig. 5b). Tributaries from Aberdare and Mt. Kenya regions recorded low pCO_2 concentrations

(median 867 ppm) compared to those from Nyambene Hills tributaries and Tana River mainstream (median 1220 ppm; ANOVA $p < 0.05$; Fig. 6b). During 2009 wet season campaign, tributaries from Mt. Kenya region recorded higher pCO_2 concentrations (t-test, $p < 0.05$), particularly those in mid-altitude catchment (1850–900 m), characterised by intensive agricultural practises. During 2009 wet season campaign, sampling at Kamburu dam was done shortly before the actual onset of the wet season. Surface waters were highly undersaturated in CO_2 during both the wet (pCO_2 = 118 ppm) and end of wet season campaigns (pCO_2 = 305 ppm). Surface waters of Masinga reservoir were similarly undersaturated in CO_2 during 2008 dry season campaign (pCO_2 from 313 to 443 ppm) but relatively oversaturated in CO_2 during end of the wet season campaign (pCO_2 from 2629 to 3389 ppm). However, pCO_2 was remarkably elevated downstream of the Masinga reservoir exit (2303 to 5204 ppm at Tana River-Masinga bridge) during all the three campaigns, but the concentrations decreased rapidly downstream (Supplement Table 1). pCO_2 showed a negative correlation with $\delta^{13}C_{DIC}$ values (Pearson correlation, $p < 0.01$, $r^2 = 0.52$; $n = 125$; Fig. 6a) during all the three campaigns.

CO_2 fluxes between the river and the atmosphere based on floating chamber measurements ranged from $-12.4\,mmol\,m^{-2}\,d^{-1}$ to $639.0\,mmol\,m^{-2}\,d^{-1}$ during the wet season campaign and from $-57.1\,mmol\,m^{-2}\,d^{-1}$ to $813.7\,mmol\,m^{-2}\,d^{-1}$ during the end of wet season campaign. The CO_2 fluxes were similar during the two seasons (Paired t-test, $p > 0.05$). Similar to pCO_2, disproportionately high water-air evasion was recorded during the end of the wet season campaign downstream of Masinga reservoir exit (Masinga bridge, $600\,mmol\,m^{-2}\,d^{-1}$). On average, Nyambene Hills tributaries recorded the highest CO_2 evasion ($-4.2\,mmol\,m^{-2}\,d^{-1}$ to $617\,mmol\,m^{-2}\,d^{-1}$) during both seasons (Fig. 7) corresponding with higher pCO_2 values (806 ppm to 4915 ppm). Generally, CO_2 fluxes showed a positive correlation with pCO_2 (Pearson correlation, $p < 0.01$, $r^2 = 0.61$, $n = 76$).

3.3 Nitrate, chlorophyll *a*, primary production and respiration measurements

Nitrate concentrations ranged from $0.4\,\mu mol\,L^{-1}$ to $146\,\mu mol\,L^{-1}$ during all the three seasons (Supplement Table 2). The concentrations increased consistently downstream during both wet season (Pearson correlation, $p < 0.01$; $r^2 = 0.75$, $n = 50$) and end of the wet season (Pearson correlation, $p < 0.01$, $r^2 = 0.50$, $n = 50$; Fig. 9b) but during the dry season nitrate did not show a systematic pattern with altitude. The highest mean concentrations ($78.6\,\mu mol\,L^{-1}$ to $96.3\,\mu mol\,L^{-1}$) were recorded in Nyambene Hills tributaries during all the three seasons.

Chlorophyll *a* concentration ranged from $0.18\,\mu g\,L^{-1}$ to $9.60\,\mu g\,L^{-1}$ with means of $2.74 \pm 2.52\,\mu g\,L^{-1}$, $1.94 \pm 1.94\,\mu g\,L^{-1}$ and $2.20 \pm 2.75\,\mu g\,L^{-1}$ during the dry season, wet season and end of the wet season respectively (Supplement Table 2). The chlorophyll *a* concentration increased consistently downstream (Pearson correlation, $p < 0.01$, $r^2 = 0.55$; $n = 117$; Fig. 8b), and values during different seasons were not significantly different (paired t-test, $p > 0.05$). Elevated chlorophyll *a* concentrations ($3.2\,\mu g\,L^{-1}$ to $20.6\,\mu g\,L^{-1}$) were recorded in the Kamburu and Masinga reservoirs during all the three sampling campaigns.

The primary production rates ranged from $0.004\,\mu mol\,L^{-1}\,h^{-1}$ to $7.38\,\mu mol\,L^{-1}\,h^{-1}$ with means of $0.42 \pm 0.46\,\mu mol\,L^{-1}\,h^{-1}$ and $0.83 \pm 1.58\,\mu mol\,L^{-1}\,h^{-1}$ for the wet and the end of the wet season campaign, respectively. The primary production rates increased consistently downstream (Pearson correlation, r^2 =0.55, $p < 0.01$, $n = 84$; Fig. 8a) during both campaigns. Disproportionately high values ranging between $10.28\,\mu mol\,L^{-1}\,h^{-1}$ to $18.28\,\mu mol\,L^{-1}\,h^{-1}$ were recorded in the Kamburu and Masinga reservoirs (Supplement Table 2). The means for different seasons were similar (paired t-test, $p > 0.05$), but Mt. Kenya and Nyambene Hills tributaries recorded significantly higher values ($0.19 \pm 0.22\,\mu mol\,L^{-1}\,h^{-1}$ and $0.79 \pm 0.45\,\mu mol\,L^{-1}\,h^{-1}$, respectively) during 2009 wet season campaign (paired t-test, $p < 0.05$) compared to 2010 end of the wet season campaign ($0.07 \pm 0.07\,\mu mol\,L^{-1}\,h^{-1}$ and $0.26 \pm 0.28\,\mu mol\,L^{-1}\,h^{-1}$, respectively).

Riverine R rates were measured only during 2009 wet season campaign and ranged from $0.20 \pm 0.07\,\mu mol\,L^{-1}\,h^{-1}$ to $3.64 \pm 0.03\,\mu mol\,L^{-1}\,h^{-1}$ with a basin-wide mean of $1.43 \pm 0.91\,\mu mol\,L^{-1}\,h^{-1}$ (Supplement Table 2). The R rates increased downstream (Pearson correlation, $p < 0.01$, $r^2 = 0.38$, $n = 33$; Fig. 9a) with Aberdares and Nyambene Hills tributaries recording the lowest mean ($0.84 \pm 0.84\,\mu mol\,L^{-1}\,h^{-1}$), Mt. Kenya tributaries intermediate ($1.37 \pm 0.90\,\mu mol\,L^{-1}\,h^{-1}$) while lower Tana River mainstream stretch the highest ($1.92 \pm 0.72\,\mu mol\,L^{-1}\,h^{-1}$). The R rates also showed a positive correlation with temperature (Pearson correlation, $r^2 = 0.46$, $p < 0.01$, $n = 33$).

3.4 Diurnal biogeochemical processes

During the diurnal cycles, water temperature fluctuated by 9.7 °C (6.9–16.6 °C), 2.1 °C (21.8–23.9 °C) and 1.5 °C (24.6–26.1 °C), while pH fluctuated by ~0.58 units (7.67–8.25), 0.14 units (6.98–7.12) and 0.05 units (7.83–7.88) at Chania stream, Masinga dam and main Tana River, respectively (Table 1). The DO saturation fluctuated by 34.6 % (89.4–124.0 %), 10.6 % (63.0–73.6 %) and 3.2 % (96.7–99.9 %) at Chania stream, Masinga dam and main Tana River, respectively (Table 1). The in situ field measurements of pH, temperature and DO increased steadily at daytime and decreased at night at Chania stream, (Fig. 10), while no discernible trends were observed at Masinga dam and Tana River mainstream.

$\delta^{18}O_{DO}$ signatures at Chania stream ranged from +22.5 ‰ to +25.5 ‰ (Supplement Table 3) with diurnal mean of $+24.0 \pm 0.8$ ‰. Although the magnitude of change was small, the values decreased during day time and increased at night time (Fig. 10). $\delta^{18}O_{DO}$ signatures showed a strong negative correlation with DO saturation (Pearson correlation, $p < 0.01$; $r^2 = 0.84$, $n = 23$; Fig. 11a). Masinga dam values (+25.4 ‰ to +28.2 ‰) showed moderate diurnal fluctuation while Tana River mainstream (+24.6 ‰ to +25.5 ‰) values did not exhibit clear diurnal fluctuations. The $\delta^{18}O_{DO}$ values at both Masinga dam and Tana mainstream remained above the atmospheric equilibrium (+24.2 ‰) during the whole diurnal cycle but values at Chania stream oscillated above and below atmospheric equilibrium though with a pronounced diurnal cycle (Fig. 10b).

The maximum $\delta^{18}O_{DO}$ value (+25.5 ‰) at Chania stream was recorded at 04:00 LT corresponding with lowest DO saturation (90.8 %). Generally, $\delta^{18}O_{DO}$ values at Chania stream were below atmospheric equilibrium (+24.2 ‰) during daytime (07:00 to 17:00 LT) and above atmospheric equilibrium at night (18:00 to 06:00 LT).

The DIC values during the diurnal cycles ranged from $0.506\,mmol\,L^{-1}$ to $0.573\,mmol\,L^{-1}$, $0.603\,mmol\,L^{-1}$ to $0.719\,mmol\,L^{-1}$ and $1.152\,mmol\,L^{-1}$ to $1.224\,mmol\,L^{-1}$ whereas $\delta^{13}C_{DIC}$ ranged from −7.2 ‰ to −5.8 ‰, −10.4 ‰ to −9.6 ‰ and −8.9 ‰ to −8.0 ‰ for Chania stream, Masinga dam and main Tana River, respectively (Supplement Table 3). The latter two sites showed a minimal $\delta^{13}C_{DIC}$ diurnal amplitude (~0.9 ‰) compared to Chania stream (1.4 ‰). $\delta^{13}C_{DIC}$ values at Chania stream typically increased during daytime and decreased at night (Fig. 12a). While the amplitudes of both DIC and $\delta^{13}C_{DIC}$ at Chania stream were small, their diurnal cycles were pronounced but showed reversed patterns (Fig. 12a). In contrast, both Masinga dam and Tana River mainstream did not exhibit clear diurnal patterns for either $\delta^{13}C_{DIC}$ or DIC. However, the DIC concentrations at main Tana River ($1.191 \pm 0.020\,mmol\,L^{-1}$) were significantly high (ANOVA, $p < 0.01$) compared to those of Chania stream ($0.547 \pm 0.021\,mmol\,L^{-1}$) and Masinga reservoir ($0.666 \pm 0.027\,mmol\,L^{-1}$).

During the diurnal cycles, pCO_2 values ranged from 174 ppm to 614 ppm, 2621 ppm to 3684 ppm and 980 ppm to 1131 ppm at Chania stream, Masinga dam and main Tana River, respectively (Supplement Table 3). pCO_2 showed systematic diurnal fluctuations at Chania stream, increasing consistently at night above the atmospheric equilibrium (385 ppm) to a maximum of 614 ppm at 22:00 LT (Fig. 13a). From 06:00 LT, the pCO_2 values started to decrease attaining a minimum plateau of ~180 ppm at 13:00 LT. In contrast, pCO_2 values at Masinga dam (2621 ppm to 3684 ppm) and Tana River mainstream (980 ppm to 1131 ppm) were consistently above atmospheric equilibrium (385 ppm) during the whole diurnal cycle with no clear diurnal fluctuation pattern. Similarly, CO_2 fluxes ranged from $-52\,mmol\,m^{-2}\,d^{-1}$ to $41\,mmol\,m^{-2}\,d^{-1}$, $95\,mmol\,m^{-2}\,d^{-1}$ to $331\,mmol\,m^{-2}\,d^{-1}$ and $2\,mmol\,m^{-2}\,d^{-1}$ to $16\,mmol\,m^{-2}\,d^{-1}$, at Chania stream, Masinga dam and Tana River mainstream, respectively (Supplement

Table 3). CO_2 fluxes and pCO_2 showed an identical diurnal pattern at Chania stream (Fig. 13a) but, CO_2 fluxes at Masinga dam and Tana River mainstream were consistently high throughout diurnal cycle and did not exhibit clear diurnal patterns.

4 Discussion

4.1 Longitudinal patterns of dissolved inorganic carbon and $\delta^{13}C_{DIC}$

In the Tana River basin, DIC generally increased downstream during all the three seasons, a strong indication of DIC build-up possibly contributed by rock weathering. This is particularly evident along the main Tana River, where DIC strongly increased downstream during all seasons (Fig. 4a), which corresponded with an increase in suspended matter (Bouillon et al., 2009; Tamooh et al., 2012). Nyambene Hills tributaries recorded exceptionally high DIC concentrations (Fig. 4a) during all three seasons, a phenomenon we associate with high rate of rock weathering. The Nyambene Hills sub-catchment is lithologically distinct from the rest of the Tana River basin, as it shows a dominance of quaternary sedimentary rocks, as opposed to the precambian or tertiary volcanic rocks dominant in the rest of the basin (King and Chapman, 1972). Overall, carbonate mineral weathering in the entire Tana River basin was reflected by strong a positive correlation between TA and sum of Ca^{2+} and Mg^{2+} solutes (Fig. 5a). Theoretically, carbonate weathering produce a ratio of 2 : 1 between TA and sum of Ca^{2+} and Mg^{2+} solutes (Barth et al., 2003). In contrast, the ratio in the present study deviated from this expected behavior with higher TA of approximately 5 : 1 ($n = 75$) recorded among tributaries and 3 : 1 ($n = 41$) along main Tana River (Fig. 5a; Supplement Table 1) indicating the additional contribution of TA from silicate weathering.

The dynamics of riverine $\delta^{13}C_{DIC}$ are primarily controlled by both in-stream and watershed processes (Finlay and Kendall, 2007). The wide range of $\delta^{13}C_{DIC}$ values recorded in the present study (−15.0 ‰ to −2.4 ‰) suggests variable carbon sources. The $\delta^{13}C_{DIC}$ values of Aberdare Range (−6.8 ± 1.6 ‰) and Mt. Kenya (−6.7 ± 2.4 ‰)

tributaries, and particularly those in high altitude regions (> 1700 m) were characterised by high $\delta^{13}C_{DIC}$ values consistent with carbonate mineral weathering. These high values may be reinforced by the fact that high altitude tributaries are characterised by fast and turbulent flows, thus enhancing CO_2 evasion to the atmosphere (equilibrium with atmospheric CO_2 yields $\delta^{13}C_{DIC}$ values of about 1 ‰). We investigated the downstream (< 1 km) gradients from the Satima springs, a high-altitude stream in Aberdare Range (3600 m). We noticed a rapid increase in $\delta^{13}C_{DIC}$ values (−20.8 ‰ to −8.8 ‰) over the first 200 m, corresponding with a fast decrease in pCO_2 (4789 ppm to 468 ppm) due to rapid CO_2 degassing to the atmosphere (Fig. 15). High $\delta^{13}C_{DIC}$ values (−4.5 ± 0.1 ‰, $n = 4$) were recorded at Masinga reservoir during the dry season campaign (Bouillon et al., 2009) consistent with CO_2 degassing combined with CO_2 consumption by primary production. The increase in water residence time at the reservoir also favours the CO_2 exchange with the atmosphere. High primary production was demonstrated by high chlorophyll *a* concentrations in the Masinga reservoir. Similar observations have been reported in other dammed rivers (Brunet et al., 2005; Zeng et al., 2011). $\delta^{13}C_{DIC}$ values were relatively depleted in main lower Tana during the three seasons. Lower $\delta^{13}C_{DIC}$ values correlated with an increase in total suspended matter (TSM) (Bouillon et al., 2009; Tamooh et al., 2012), suggesting that degradation of laterally derived organic matter plays an important role in controlling $\delta^{13}C_{DIC}$ values along main lower Tana River. When excluding values from Nyambene Hills tributaries, the negative relationship between $\delta^{13}C_{DIC}$ values and DIC concentration (Pearson correlation, $p < 0.01$, $r^2 = 0.62$, $n = 39$) and the positive correlation between $\delta^{13}C_{DIC}$ values and DO (Pearson correlation, $p < 0.01$, $r^2 = 0.52$, $n = 39$) during wet season campaign further confirms the evidence of organic matter oxidation consistent with downstream increase in dissolved organic carbon (Tamooh et al., 2012).

4.2 Factors regulating pCO_2 and CO_2 fluxes

As reported for other tropical rivers (Richey et al., 2002; Mayorga et al., 2005; Aufdenkampe et al., 2011), the Tana River was generally supersaturated in CO_2 with respect to atmospheric equilibrium (385 ppm). This was the case during all the three seasons. The overall pCO_2 median for Tana River (1002 ppm) is however relatively low compared to global median of ∼ 3600 ppm and ∼ 4300 ppm for tropical rivers and stream, respectively (Aufdenkampe et al., 2011). The Tana River tributaries at high altitudes were characterised by pCO_2 concentrations, which were relatively low compared to other tropical high altitude streams e.g. 11000 ppm to 25000 ppm for Amazon headwaters (Davidson et al., 2010). One possible explanation is relatively low in-stream respiration, as Tana River headwater streams are characterized by low suspended sediment (Bouillon et al., 2009; Tamooh et al., 2012) and low temperatures, resulting in a lower CO_2 production from organic matter degradation. In addition, the CO_2 carried by groundwater input rapidly degasses into atmosphere, as we clearly observed in the Aberdares headwaters. The CO_2 from groundwater at Satima springs rapidly degassed (4789 ppm to 468 ppm) with increasing distance from the spring source (Fig. 14), resulting in ∼ 90 % CO_2 evasion over a distance of a few 100 m. Similar observations have been reported from both temperate headwater streams in northeast Vermont, USA and Sweden (Doctor et al., 2008; Wallin et al., 2012) as well as in tropical headwater streams in Amazon basin (Johnson et al., 2008; Davidson et al., 2010), thus depicting small streams as hotspots for CO_2 evasion. Further, we observed a strong coupling between isotopic signatures of DIC andpCO_2 where $\delta^{13}C_{DIC}$ values (−20.8 ‰ to −8.8 ‰) became rapidly enriched downstream, thus providing further evidence of rapid degassing downstream from groundwater inputs (Fig. 14). Some studies in tropical systems attribute supersaturation of dissolved CO_2 (pCO_2) in groundwater to production of carbon dioxide (CO_2) from soils, thus returning terrestrially fixed carbon back to the atmosphere (Johnson et al., 2008; Davidson et al., 2010). In contrast to Aberdare and Mt. Kenya streams, Nyambene Hills tributaries recorded relatively high

pCO_2 concentrations (median 1377 ppm, $n = 12$; Fig. 6b) and high CO_2 effluxes (median ∼ 260 mmol m^{-2} d^{-1}; Fig. 7; Supplement Table 1), notably in Murera and Mutundu tributaries during both wet and end of wet season campaigns. However, Nyambene Hills tributaries were characterized by a cover of high organic matter on the river bed possibly contributing to additional generation of CO_2 through respiration. This way, Nyambene Hills sub-catchment emerges as a major hotspot for CO_2 emissions within the Tana River basin.

Primary production strongly controlled the pCO_2 dynamics in the reservoirs as demonstrated by low pCO_2 values during the dry season at Masinga reservoir (313 to 443 ppm) and Kamburu dam during both wet (118 ppm) and end of the wet season (305 ppm) campaigns (Supplement Table 1). Low turbidity coupled with high water residence time and temperatures (∼ 30 °C) in the reservoirs enhanced phytoplankton production, thus consuming CO_2. In contrast, the depth profile data obtained at Masinga dam (up to 15 m deep) recorded consistently high pCO_2 values (3385 ± 212 ppm, $n = 5$) during the end of the wet season campaign, suggesting the dam water was well mixed owing to the fact that this sampling campaign coincided with an unusual dam infilling (following high precipitation in headwaters) and excess outflow at the spillway, thus enhancing upwelling process. Furthermore, a maximal pCO_2 value (5059 ppm) was recorded at 20 m depth (Supplement Table 1). Conversely, Kamburu dam recorded highly stratified pCO_2 values during both wet season (118 ppm at surface waters and 2556 ppm at 20 m depth) and end of the wet season campaigns (305 ppm at surface waters and 3270 ppm at 20 m depth) (Supplement Table 1). In addition, consistently high pCO_2 values (up to 5204 ppm) and CO_2 flux (600 mmol m^{-2} d^{-1}) were recorded downstream of Masinga reservoir exit (Masinga bridge), a phenomenon we attribute to release of hypolimnetic, CO_2 rich water. However, the CO_2 degassed rapidly < 5 km downstream where we observe ∼ 90 % of CO_2 being degassed before reaching the entrance of Kamburu dam (Supplement Table 1). This suggests that the Masinga reservoir contributes significantly to CO_2 emission downstream. This is consistent with observations reported in some tropical reservoirs where CO_2 flux ranging from

412 mmol m^{-2} d^{-1} to 1494 mmol m^{-2} d^{-1} were recorded immediately downstream of the reservoirs (Guérin et al., 2006; Abril et al., 2005).

While different in-stream and watershed processes regulate riverine pCO_2 dynamics, organic matter respiration within the river seemed to be the major controlling process in the main Tana River as reflected by high pCO_2 values during 2009 wet season campaign, which was characterized by high suspended sediment and dissolved organic carbon particularly in lower Tana River mainstream thus, fuelling in-stream respiration (Tamooh et al., 2012). This is further corroborated by the general negative correlation observed between $\delta^{13}C_{DIC}$ values and pCO_2 values (Fig. 6a) In-stream processing and decomposition of terrestrially-derived organic carbon have been reported to primarily regulate CO_2 evasion in most large tropical rivers (Richey et al., 2002; Mayorga et al., 2005).

4.3 Dynamics of aquatic metabolism

River metabolism is primarily influenced by availability of light and nutrients, temperature, and organic matter subsidies. Both primary production rates and chlorophyll *a* concentrations increased consistently downstream in Tana River basin (Fig. 8), contrary to the expectation, as the turbidity increased downstream (Bouillon et al., 2009; Tamooh et al., 2012). However, primary production rates here are based on incubations of surface water within the euphotic zone (~ 0.5 m deep) and do not represent depth integrated values (deeper in the water water column light is obviously extinct). The downstream increase in primary production can be attributed to higher temperatures coupled with higher water residence time in the lower main Tana River. In addition, during the wet season, the nitrate concentrations increased downstream (Pearson correlation, r^2 =0.75, $p < 0.01$, $n = 50$; Fig. 9b), particularly along the lower main Tana River, thus potentially enhancing primary production. This counterintuitive observation of high productivity in turbid river has also been reported for some large temperate rivers, such as the Mississippi (Kendall et al., 2001; Delong and Thorp, 2006) and

Meuse (Descy and Gosselain, 1994), as well as in the White Nile (Sinada and Karim, 1984). While most headwater tributaries are characterized by low suspended matter, primary production rates were low owing to nutrient limitation, low temperature and high stream flow velocity; factors unfavourable for efficient phytoplankton production. Generally, primary production in tropical rivers has been reported to be quite variable ranging from lows of 10–200 mg C m^{-2} d^{-1} to over 1000 mg C m^{-2} d^{-1} in relatively unpolluted systems but can exceed 6000 mg C m^{-2} d^{-1} in polluted systems (Davies et al., 2008).

The mean river depth between Kora bridge and the Tana River mouth during wet season ranges between 2.0 m and 3.0 m while the average respiration rate along the same stretch was ~ 1.92 ± 0.72 µmol L^{-1} h^{-1}. This would translate to a depth-integrated pelagic respiration ranging between 92 mmol m^{-2} d^{-1} to 138 mmol m^{-2} d^{-1}, while the median CO_2 efflux was 156 mmol C m^{-2} d^{-1} (Table 2; Fig. 7a). Assuming the net primary production is negligible, this suggests that the bulk of CO_2 evasion (59 % to 88 %) along the lower Tana mainstream can be accounted for by in-stream respiration (Table 2; Fig. 7a). These estimates are based on the general assumption the that respiration quotient between O_2 and CO_2 is unity. Similar observations have been reported in the Amazon basin where in-stream respiration was highly variable, but could account for up to ~ 100 % of the CO_2 evasion in some rivers (Ellis et al., 2012).

In contrast, most headwater tributaries in Tana River basin are shallow (~ 0.5–1 m deep) with depth-integrated respiration rates ranging between ~ 10 mmol m^{-2} d^{-1} to 33 mmol m^{-2} d^{-1} while the median CO_2 fluxes ranged between 38 mmol m^{-2} d^{-1} and 260 mmol m^{-2} d^{-1} (Table 2; Fig. 7a). This implies that in-stream respiration accounts for a smaller fraction of total CO_2 evasion (4 % to 52 %) in the studied tributaries compared to the main Tana River. This is particularly the case for the Nyambene Hills tributaries, whose pelagic respiration accounts for only 4 % to 8 % of total CO_2 evasion (Table 2; Fig. 7a). This suggests the excess bulk CO_2 evasion must be sustained by other processes such as inputs of groundwater, soil and root respiration, or in-stream benthic respiration. The latter hypothesis is in agreement with the fact that most Nyambene

Hills tributaries were characterized by high organic matter on the bottom of the river bed possibly fuelling respiration.

4.4 Factors regulating diurnal variations in surface water biogeochemistry

Diurnal fluctuations of biogeochemical variables were substantial in the Chania headwater stream, moderate at Masinga reservoir, and not detectable within the lower main Tana. Dissolved oxygen was supersaturated with respect to atmospheric equilibrium at headwater Chania stream reaching a maximum value of 124.0 % at daytime (11:00 LT) and minimum saturation of 89.4 % at 06:00 LT, shortly before sunrise. Similarly, the pH increased at daytime (indicative of CO_2 consumption by photosynthesis) and a decreased at night (indicative of CO_2 release by respiration). These patterns were absent at both Masinga reservoir dam and lower main Tana River, where biogeochemical parameters remained nearly constant during the whole diurnal cycle. Masinga dam surface waters were particularly under-saturated in DO (63.0 % to 73.6 %; Table 1) suggesting dominance of respiration and net heterotrophy. The absence and/or small fluctuation of DO at Masinga and Tana River mainstream may be attributed to high suspended loads (Bouillon et al., 2009; Tamooh et al., 2012) which attenuates photosynthetic light, as opposed to headwater Chania stream characterised by low suspended matter.

The $\delta^{18}O_{DO}$ signatures fluctuated by ~ 3.0 ‰, 2.8 ‰, and 0.9 ‰ at headwater Chania stream, Masinga reservoir and main Tana River respectively. The signatures at Chania stream were isotopically light at daytime and enriched at night although the fluctuations oscillated slightly below and above the atmospheric equilibrium (+24.2 ‰). This suggests that aquatic *P* dominated riverine biological activities during the day but reversed to *R* dominance at night. This was clearly demonstrated by $\delta^{18}O_{DO}$ signatures that were consistently below atmospheric equilibrium at daytime as aquatic photoautotrophs produced isotopically light DO while at night time, *R* consumed preferentially light DO leaving isotopically enriched residual DO with values above atmospheric equilibrium. Similar observations have been reported in small streams elsewhere (Parker

et al., 2005, 2010; Waldron et al., 2007; Gammons et al., 2011; Nimick et al., 2011). In contrast, Masinga dam and Tana River mainstream $\delta^{18}O_{DO}$ signatures were consistently above atmospheric equilibrium (+24.2 ‰) suggesting the two sites were dominated by *R* and thus, predominantly heterotrophic during the whole diurnal period.

Precipitation and dissolution of $CaCO_3$ in freshwaters can be deduced from changes in TA (e.g. McConnaughey et al., 1994). In Masinga dam and Tana River mainstream, TA did not show a distinct pattern during the diurnal cycle. In Chania stream, the TA values followed a regular pattern with a decrease from 01:00 LT to 13:00 LT of about 0.035 mmol L^{-1}, (Fig. 13b) inconsistent with the one expected from daily cycles of precipitation/dissolution of $CaCO_3$ (increase of TA during night-time and decrease of TA during day-time, de Montety et al., 2011; Gammons et al., 2011). The changes of TA in Chania stream followed those of conductivity suggesting overall changes in the chemistry of flowing waters, rather than in-stream processes affecting TA. We conclude that changes in DIC can be ascribed to *P* and *R* and that precipitation/dissolution of $CaCO_3$ was not a major process contributing to daily changes of DIC. The DIC concentration showed a fluctuation of ~ 0.067 mmol L^{-1}, 0.116 mmol L^{-1}, and 0.072 mmol L^{-1} at Chania stream, Masinga reservoir and main Tana River, respectively. However, DIC concentrations and $\delta^{13}C_{DIC}$ values showed a strong inverse relationship (Pearson correlation, $p < 0.01$; $r^2 = 0.87$; $n = 22$; Fig. 11c) characterized by pronounced diurnal cycle at Chania stream only. DIC concentrations at Chania stream increased at night due to aquatic community respiration and decreased at daytime as aquatic prototroph consume CO_2. Studies elsewhere have reported substantial diurnal changes in DIC concentrations ranging from 0.300 mmol L^{-1} to 0.420 mmol L^{-1} (Poulson and Sullivan, 2010; Gammons et al., 2011) with a record fluctuation of ~ 1.133 mmol L^{-1} reported by Parker et al. (2010). However, this large diurnal change in DIC concentration is reported to have been driven by unique calcite precipitation and not in-stream *P* or *R* (Gammons et al., 2007; Nimick et al., 2011).

Similarly, $\delta^{13}C_{DIC}$ values at Chania stream showed a modest fluctuation of ~ 1.4 ‰ with signatures increasing at daytime as $^{12}CO_2$ was preferentially utilised by aquatic

periphytic phototrophs at a faster rate than $^{13}CO_2$. At night, $\delta^{13}C_{DIC}$ signatures were isotopically depleted as CO_2 was released as a result of aquatic community respiration. In contrast, $\delta^{13}C_{DIC}$ in Masinga dam and main Tana River showed minor fluctuations (~ 0.8 ‰ and 0.9 ‰, respectively) and did not exhibit systematic diurnal patterns. The small fluctuations of $\delta^{13}C_{DIC}$ values at Masinga reservoir and main Tana River (Supplement Table 3) indicate dominance of respiration compared to *P* suggesting the two sites are predominantly heterotrophic.

Chania stream showed strong diurnal cycles for both pCO_2, and CO_2 fluxes with in-stream *P* and *R* as the major drivers as reflected by a strong negative correlation between DO and pCO_2 (Pearson correlation, $p < 0.01$; $r^2 = 0.74$; Fig. 11e). In contrast, pCO_2 concentrations at Masinga dam (2621 ppm to 3684 ppm) and main Tana River (980 ppm to 1131 ppm) were consistently above atmospheric equilibrium (385 ppm) suggesting the two sites were sources of CO_2 to the atmosphere during the whole diurnal period. Water to air CO_2 fluxes at Masinga reservoir (95 mmol CO_2 m^{-2} d^{-1} to 331 mmol CO_2 m^{-2} d^{-1}) and main Tana River (2 mmol CO_2 m^{-2} d^{-1} to 16 mmol CO_2 m^{-2} d^{-1}) similarly confirm that these two sites are net heterotrophic.

While the general observation is that in-stream *P* and *R* control biogeochemical processes in Chania stream, it is worth mentioning that *P* is largely driven by periphyton as opposed to phytoplankton as demonstrated by low *P* and chlorophyll *a* in headwaters tributaries.

5 Conclusions

While the wide range of $\delta^{13}C_{DIC}$ values (−15.0 ‰ to −2.4 ‰) in the Tana River basin suggests variable DIC sources, the primary process regulating of DIC concentrations is weathering as clearly demonstrated by a strong correlation between TA and sum of Ca^{2+} and Mg^{2+} concentration. However, Nyambene Hills subcatchment is lithologically

distinct from the rest of the basin as reflected by its systematically high TA during all seasons. Global syntheses suggest that streams are generally characterized by higher pCO_2 than large rivers, but our data show the opposite pattern with higher concentrations of CO_2 recorded in main Tana River compared to headwater streams. Chlorophyll *a* and primary production increased consistently downstream contrary to what could be expected from the RCC and from high TSM concentrations, due to favourable conditions for phytoplankton development such as high nutrients, temperature and water residence time. In-stream *R* in lower main Tana River accounted for the bulk of total CO_2 evasion (59 % to 89 %) to the atmosphere, while it could only account for 4 % to 52 % of CO_2 evasion in headwaters, thus pointing toward greater contributions by other watershed processes or in-stream processes such as benthic respiration. Focusing on a depth integrated primary production measurement in future is critical in order to give an accurate estimate of $P : R$ ratios for Tana River. The diurnal biogeochemical fluctuations were substantial in headwater streams, moderate in Masinga reservoir and not detectable at Tana River mainstream implying Masinga reservoir and Tana River mainstream. However, the timing for Masinga reservoir sampling was unusual due to infilling of the reservoir resulting in high water turbulence associated with high turbidity and vertical mixing of water, thus diurnal biogeochemical fluctuations at Masinga dam were not representative of a typical situation. Hence, there is need to focus on a more representative diurnal sampling in the reservoirs in future studies particularly during dry season when phytoplankton production is expected to be significant.

Supplementary material related to this article is available online at: http://www.biogeosciences-discuss.net/10/5175/2013/bgd-10-5175-2013-supplement.pdf.

Acknowledgements. Funding for this work was provided by the Research Foundation Flanders (FWO-Vlaanderen, project G.0651.09 and travel grants to F. T., K. V. d. M., and S. B), and the European Research Council (ERC-StG 24002, AFRIVAL-African river basins: Catchment-scale carbon fluxes and transformations, http://ees.kuleuven.be/project/afrival/). AVB is a research associate at the FRS-FNRS. We thank Pieter van Rijswijk (NIOZ), Peter van Breugel (NIOZ), and Marc-Vincent Commarieu (ULg) for technical and laboratory assistance, Kenya Wildlife Service for logistical support during sampling.

References

Abril, G., Etcheber, H., Delille, B., Frankignoulle, M., and Borges, A. V.: Carbonate dissolution in the turbid and eutrophic Loire estuary, Mar. Ecol-Prog. Ser., 259, 129–138, 2003.

Abril, G., Guérin, F., Richard, S., Delmas, R., Galy-Lacaux, C., Gosse, P., Tremblay, A., Varfalvy, L., dos Santos, M. A., and Matvienko, B.: Carbon dioxide and methane emissions and the carbon budget of a 10-year old tropical reservoir (Petit Saut, French Guiana), Global Biogeochem. Cy., 19, GB4007, doi:10.1029/2005GB002457, 2005.

Amiotte-Suchet, P., Aubert, D., Probst, J. L., Gauthier-Lafaye, F., Probst, A., Andreux, F., and Viville. D.: δ^{13}C pattern of dissolved inorganic carbon in a small granitic catchment: the Strengbach case study (Vosges mountains, France), Chem. Geol., 159, 129–145, 1999.

Aufdenkampe, K. A., Mayorga, E., Raymond, A P., Melack, M J., Doney, C. S., Alin, R. S., Aalto, E. R., and Yoo, K.: Riverine coupling of biogeochemical cycles between land, oceans, and atmosphere, Front. Ecol. Environ., 9, 53–60, 2011.

Barth, J. A. C., Cronin, A. A., Dunlop, J., and Kalin, R. M.: Influence of carbonates on the riverine carbon cycle in an anthropogenically dominated catchment basin: evidence from major elements and stable carbon isotopes in the Lagan River (N. Ireland), Chem. Geol., 200, 203–216, 2003.

Bouillon, S., Abril, G., Borges, A. V., Dehairs, F., Govers, G., Hughes, H. J., Merckx, R., Meysman, F. J. R., Nyunja, J., Osburn, C., and Middelburg, J. J.: Distribution, origin and cycling of carbon in the Tana River (Kenya): a dry season basin-scale survey from headwaters to the delta, Biogeosciences, 6, 2475–2493, doi:10.5194/bg-6-2475-2009, 2009.

Bouwman, A. F., Bierkens, M. F. P., Griffioen, J., Hefting, M. M., Middelburg, J. J., Middelkoop, H., and Slomp, C. P.: Nutrient dynamics, transfer and retention along the aquatic

continuum from land to ocean: towards integration of ecological and biogeochemical models, Biogeosciences, 10, 1–22, doi:10.5194/bg-10-1-2013, 2013.

Brown, T. and Schneider, H.: From plot to basin: the scale problem in studies of soil erosion and sediment yield, in: The Sustainable Management of Tropical Catchments, edited by: Harper, D. and Brown, T., John Wiley and Sons, Chichester, England, 1998.

Brunet, F., Gaiero, D., Probst, J. L., Depetris, P. J., Gauthier, Lafaye, F., and Stille, P.: δ^{13}C tracing of dissolved inorganic carbon sources in Patagonian rivers (Argentina), Hydrol. Process., 19, 3321–3344, 2005.

Brunet, F., Dubois, K., Veizer, J., Nkoue Ndondo, G. R., Ndam Ngoupayou, J. R., Boeglin, J. L., and Probst, J. L.: Terrestrial and fluvial carbon fluxes in a tropical watershed: Nyong Basin, Cameroon, Chem. Geol., 265, 563–572, 2009.

Bullen, T. D. and Kendall, C.: Tracing of weathering reactions and water flowpaths: a multi-isotope approach, in: Isotope Tracers in Catchment Hydrology, edited by: Kendall, C. and McDonnell, J. J., Elsevier, Amsterdam, 611–646, 1998.

Butman, D. and Raymond, P. A.: Significant efflux of carbon dioxide from streams and rivers in the United States, Nat. Geosci., 4, 839–842, doi:10.1038/ngeo1294, 2011.

Cole, J. J. and Caraco, N. F.: Carbon in catchments: connecting terrestrial carbon losses with aquatic metabolism, Mar. Freshwater Res., 52, 101–110, 2001.

Cole, J. J., Prairie, Y. T., Caraco, N. F., McDowell, W. H., Tranvik, L. J., Striegl, R. G., Duarte, C. M., Kortelainen, P., Downing, J. A., Middelburg, J. J., and Melack, J.: Plumbing the global carbon cycle: integrating inland waters into the terrestrial carbon budget, Ecosystems, 10, 171–184, 2007.

Dauchez, S., Legendre, L., and Fortier, L.: Assessment of simultaneous uptake of nitrogenous nutrients (^{15}N) and inorganic carbon (^{13}C) by natural phytoplankton populations, Mar. Biol., 123, 651–666, 1995.

Davies, P. M., Bunn, E. S., and Hamilton, K. S: Primary production in tropical streams and rivers, in: Aquatic Ecosystems: Tropical Stream Ecology, edited by: Dudgeon, D., Elsevier Science, London, UK, 23–42, 2008.

Davidson, E. A., Figueiredo, R. O., Markewitz, D., and Aufdenkampe, A. K.: Dissolved CO_2 in small catchment streams of eastern Amazonia: a minor pathway of terrestrial carbon loss, J. Geophys. Res., 115, G04005, doi:10.1029/2009JG001202, 2010.

Delong, M. D. and Thorp, J. H.: Significance of instream autotrophs in trophic dynamics of the Upper Mississippi River, Oecologia, 147, 76–85, 2006.

de Montety V., Martin, J. B., Cohen, M. J., Foster, C., and Kurz, M. J.: Influence of diel biogeochemical cycles on carbonate equilibrium in a karst river, Chem. Geol., 283, 31–43, 2011.
Descy, J.- P. and Gosselain, V.: Development and ecological importance of phytoplankton in a large lowland river (River Meuse, Belgium), Hydrobiologia, 289, 139–155, 1994.
Doctor, D. H., Kendall, C., Sebestyen, S. D., Shanley, J. B., Ohte, N., and Boyer, E. W.: Carbon isotope fractionation of dissolved inorganic carbon (DIC) due to outgassing of carbon dioxide from a headwater stream, Hydrol. Process., 22, 2410–2423, 2008.
Dunne, T. and Ongweny, G. S. O.: A new estimate of sedimentation rates on the upper Tana River, The Kenyan Geographer, 2, 109–126, 1976.
Ellis, E. E., Richey, J. E., Aufdenkampe, A. K., Krusche, A. V., Quay, P. D., Salimon, C., and Cunha, H. B.: Factors controlling water-column respiration in rivers of the central and southwestern Amazon Basin, Limnol. Oceanogr., 57, 527–540, 2012.
Finlay, J. C.: Controls of streamwater dissolved inorganic carbon dynamics in a forested watershed, Biogeochemistry, 62, 231–252, 2003.
Finlay, J. C. and Kendall, C.: Stable isotope tracing of temporal and spatial variability in organic matter sources to freshwater ecosystems, in: Stable Isotopes in Ecology and Environmental Science, 2nd edn., edited by: Michener, R. H. and Lajtha, K., Blackwell Publishing, Malden, USA, 283–333, 2007.
Gammons, C. H., Grant, T. M., Nimick, D. A., Parker, S. R., and DeGrandpre, M. D.: Diel changes in water chemistry in an arsenic-rich stream and treatment-pond system, Sci. Total Environ., 384, 433–451, 2007.
Gammons, C. H., Babcock, J., Parker, S. R., and Poulson, S. R.: Diel cycling and stable isotopes of dissolved oxygen, dissolved inorganic carbon, and nitrogenous species in a hypereutrophic stream, Chem. Geol., 283, 44–55, 2011.
Gillikin, D. P. and Bouillon, S.: Determination of δ^{18}O of water and δ^{13}C of dissolved inorganic carbon using a simple modification of an elemental analyzer – isotope ratio mass spectrometer (EA-IRMS): an evaluation, Rapid Commun. Mass Sp., 21, 1475–1478, 2007.
GOK-TARDA: Tana Delta Irrigation Project-Feasibility Study, vol. III – Hydrology, River Morphology and Flood Plain Hydraulics, Haskoning-Royal Dutch Consulting Engineers and Architects, Netherlands and Mwenge International Associates Ltd, Nairobi, Kenya, 1982.
Guérin, F., Abril, G., Richard, S., Burban, B., Reynouard, C., Seyler, P., and Delmas, R.: Methane and carbon dioxide emissions from tropical reservoirs: significance of downstream rivers, Geophys. Res. Lett., 33, L21407, doi:10.1029/2006GL027929, 2006.

Hendricks, M. B., Bender, M. L., Barnett, B. A., Strutton, P., and Chavez, F. P.: Triple isotope composition of dissolved O_2 in the equatorial Pacific: a tracer of mixing, production, and respiration, J. Geophys. Res., 110, C12021, doi:10.1029/2004JC002735, 2005.
Johnson, M. S., Lehmann, J., Riha, S. J., Krusche, A. V., Richey, J. E., Ometto, J. P. H. B., and Couto, E. G.: CO_2 efflux from Amazonian headwater streams represents a significant fate for deep soil respiration, Geophys. Res. Lett., 35, L17401, doi:10.1029/2008GL034619, 2008.
Kempe, S.: Sinks of anthropogenically enhanced carbon cycle in surface fresh waters, J. Geophys. Res., 89, 4657–4676, 1984.
Kendall, C., Silva, S. R., and Kelly, V. J.: Carbon and nitrogen isotopic compositions of particulate organic matter in four large river systems across the United States, Hydrol. Process., 15, 1301–1346, 2001.
King, B. C. and Chapman, G. R.: Volcanism of the Kenyan rift valley, Philos. T. R. Soc. S.-A, 271, 185–208, doi:10.1098/rsta.1972.0006, 1972.
Maingi, J. K. and Marsh, S. E.: Quantifying hydrologic impacts following dam construction along the Tana River, Kenya, J. Arid Environ., 50, 53–79, 2002.
Maiolini, B. and Bruno, M. C.: The River Continuum Concept revisited: Lessons from the Alps, Alpine Space – Man and Environment, 3: 67–76, ISBN 978-3-902571-33-5, 2007.
Mayorga, E., Aufdenkampe, A. K., Masiello, C. A., Krusche, A. V., Hedges, J. I., Quay, P. D., Richey, J. E., and Brown, T. A.: Young organic matter as a source of carbon dioxide outgassing from Amazonian Rivers, Nature, 436, 538–541, 2005.
McConnaughey, T. A., LaBaugh, J. W., Rosenberry, D. O., Striegl, R. G., Reddy, M. M., Schuster, P. F., and Carter, V.: Carbon budget for a groundwater-fed lake: calcification supports summer photosynthesis, Limnol. Oceanogr., 39, 1319–1332, 1994.
Millero, F. J.: The thermodynamics of the carbonate system in seawater, Geochim. Cosmochim. Ac., 43, 1651–1661, 1979.
Milliman, D. J. and Farnsworth, L. K.: River Discharge to the Coastal Ocean: a Global Synthesis, Cambridge University Press, 2011.
Nimick, D. A., Gammons, C. H., and Parker, S. R.: Diel biogeochemical processes and their effect on the aqueous chemistry of streams: a review, Chem. Geol., 283, 3–17, 2011.
Odum, H. T.: Primary production in flowing waters, Limnol. Oceanogr., 1, 102–117, 1956.
Parker, S. R., Poulson, S. R., Gammons, C. H., and Degrandpre, M. D.: Biogeochemical controls on diel cycling of stable isotopes of dissolved O_2 and dissolved inorganic carbon in the Big Hole River, Montana, Environ. Sci. Technol., 39, 7134–7140, doi:10.1021/es0505595, 2005.

Parker, S. R., Gammons, C. H., Poulson, S. R., DeGrandpre, M. D., Weyer, C. L., Smith, M. G., Babcock, J. N., and Oba, Y.: Diel behavior of stable isotopes of dissolved oxygen and dissolved inorganic carbon in rivers over a range of trophic conditions, and in a mesocosm experiment, Chem. Geol., 269, 21–31, 2010.

Poulson, S. R. and Sullivan, A. B.: Assessment of diel chemical and isotopic techniques to investigate biogeochemical cycles in the upper Klamath River, Oregon, USA, Chem. Geol., 269, 3–11, 2010.

Richey, J. E., Melack, J. M., Aufdenkampe, A. K, Ballester, V. M., and Hess, L.: Outgassing from Amazonian rivers and wetlands as a large tropical source of atmospheric CO_2, Nature, 416, 617–620, 2002.

Sinada, F. and Karim, A. G. A.: Primary production and respiration of the phytoplankton in the Blue and White Niles at Khartoum, Hydrobiologia, 110, 57–59, 1984.

Tamooh, F., Van den Meersche, K., Meysman, F., Marwick, T. R., Borges, A. V., Merckx, R., Dehairs, F., Schmidt, S., Nyunja, J., and Bouillon, S.: Distribution and origin of suspended matter and organic carbon pools in the Tana River Basin, Kenya, Biogeosciences, 9, 2905–2920, doi:10.5194/bg-9-2905-2012, 2012.

Telmer, K. and Veizer, J.: Carbon fluxes, pCO_2 and substrate weathering in a large northern river basin, Canada: carbon isotope perspectives, Chem. Geol., 159, 61–86, 1999.

Vannote, R. L., Minshall, G. W., Cummins, K. W., Sedell, J. R., and Cushing, C. E.: The river continuum concept, Can. J. Fish. Aquat. Sci., 37, 130–137, 1980.

Venkiteswaran, J. J., Wassenaar, L. I., and Schiff, S. L.: Dynamics of dissolved oxygen isotopic ratios: a transient model to quantify primary production, community respiration, and air–water exchange in aquatic ecosystems, Oecologia, 153, 385–398, 2007.

Wallin, M. B., Grabs, T., Buffam, I., Laudon, H., A., Mats, G. O., and Bishop, K.: Evasion of CO_2 from streams – the dominant component of the carbon export through the aquatic conduit in a boreal landscape, Glob. Change Biol., 19, 785–797, doi:10.1111/gcb.12083, 2012.

Waldron, S., Scott, E. M., and Soulsby, C.: Stable isotope analysis reveals lower-order river dissolved inorganic carbon pools are highly dynamic, Environ. Sci. Technol., 41, 6156–6162. 2007.

Zeng, F- W., Masiello C. A., and Hockaday, W. C.: Controls on the origin and cycling of riverine dissolved inorganic carbon in the Brazos River, Texas, Biogeochemistry, 104, 275–291, doi:10.1007/s10533-010-9501-y, 2011.

Table 1. A summary of physico-chemical parameters range where 24-h sampling was performed.

Site	Sampling date	Mean depth (m)	DO (%)	pH	T (°C)	SC ($\mu S\,cm^{-1}$)
Chania stream	12 Sep 2009	0.5	98.4–124.0	7.67–8.25	6.9–16.6	50–53
Masinga Dam	27 Jun 2010	20	63.0–73.6	6.98–7.12	22.0–23.4	71–75
Tana mainstream	20 Jul 2010	3	96.7–99.9	7.83–7.88	24.6–25.8	134–137

Range for each parameter: DO = Dissolved Oxygen saturation; pH; T = Temperature; SC = Specific Conductivity

Table 2. Comparison between CO_2 flux evasion and depth-integrated R during 2009 wet season campaign.

Site	Mean river depth (m)	Median CO_2 flux ($mmol\,C\,m^{-2}\,d^{-1}$)	Depth integrated R ($mmol\,C\,m^{-2}\,d^{-1}$)	% of CO_2 evasion accounted by R
Aberdares streams	~ 0.5–1.0	38	10–20	26–52
Mt. Kenya streams	~ 0.5–1.0	85	16–33	19–39
Nyambene Hills streams	~ 0.5–1.0	260	11–21	4–8
Tana River mainstream	~ 2.0–3.0	156	92–138	59–88

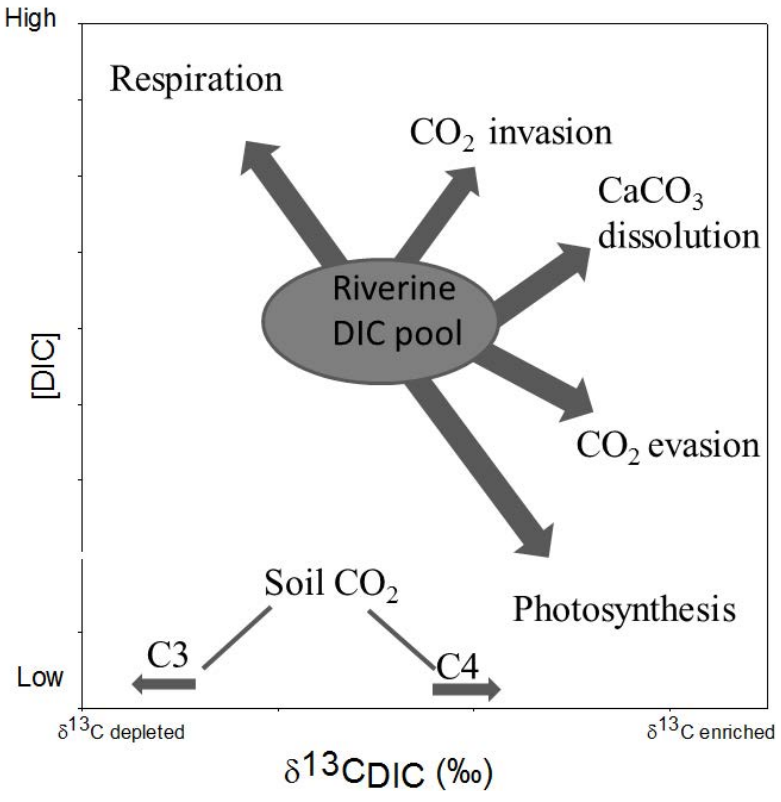

Fig. 1. Conceptual model showing the main watershed and in-stream biogeochemical processes controlling riverine DIC concentration and $\delta^{13}C_{DIC}$ signatures.

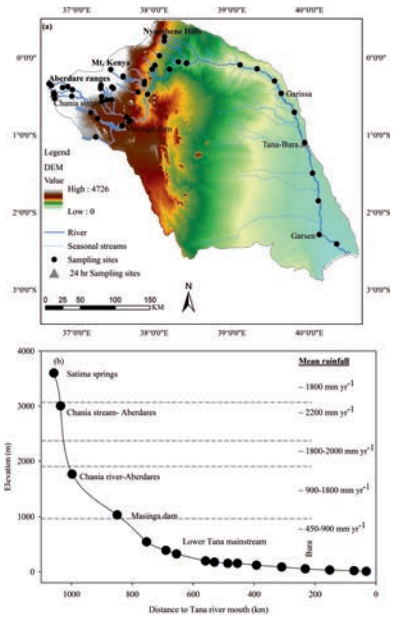

Fig. 2. (a) Digital Elevation Model (DEM) of the Tana River Basin, which consists of two main geographical units, the Tana headwaters and the main lower Tana. The 57 sampling sites are indicated by black dots, **(b)** Profile of the Tana River from headwaters to Tana mouth. Sampling stations for the lower Tana River are indicated, as well as a selected number of headwater sampling sites to show their overall position. Note, Chania stream, Masinga dam and Tana-Bura are 24 h cycle sampling sites.

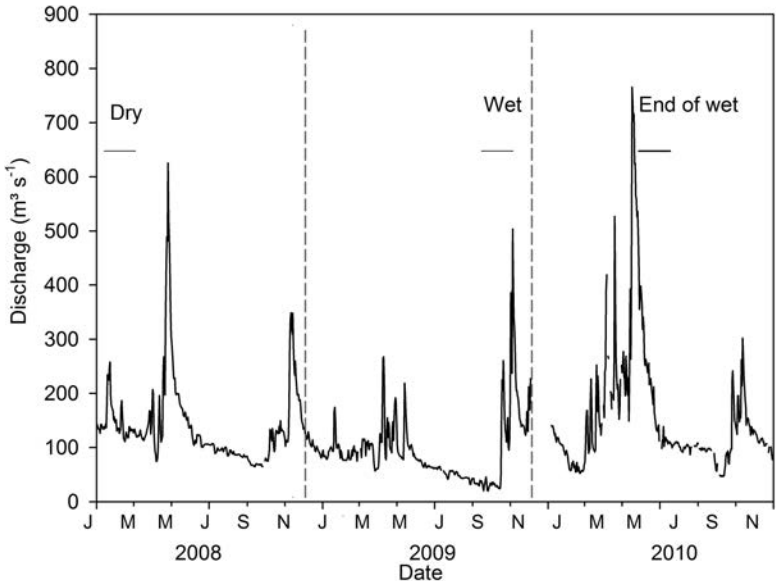

Fig. 3. Discharge measurements for the Tana River (2008–2010) as recorded at Garissa station. (Data source: Water Resource Management Authority). Horizontal lines indicate the duration of the three field investigations while vertical dashed lines separate different years.

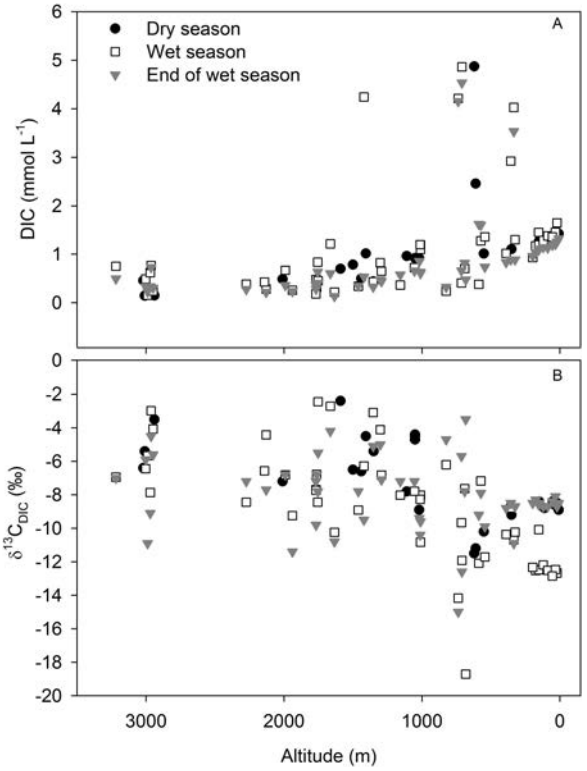

Fig. 4. Altitudinal profiles of **(A)** dissolved inorganic carbon concentrations, and **(B)** $\delta^{13}C_{DIC}$ along Tana River Basin during three sampling seasons.

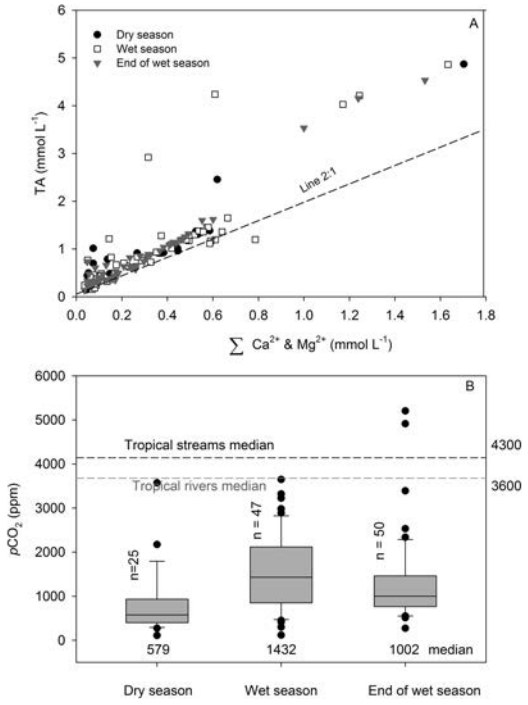

Fig. 5. (A) TA vs. sum of Ca^{2+} and Mg^{2+} concentrations along Tana River Basin. Line 2 : 1 represents the ratio of TA: Ca^{2+} and Mg^{2+} for carbonate weathering, **(B)** Boxplots of pCO_2 during the three sampling campaigns. The *center line*, *box extent*, *error bars*, and *dots* denote the 50th, 25th and 75th, 10th and 90th, and outliers of estimates. Horizontal dashed lines represent tropical medians for rivers and streams (Aufdenkampe et al., 2011).

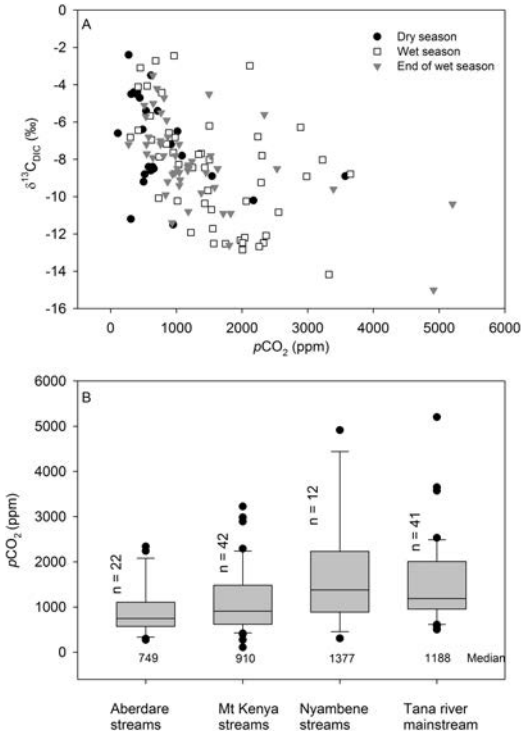

Fig. 6. (A) Plot of $\delta^{13}C_{DIC}$ vs. pCO_2 along Tana River Basin, **(B)** Boxplots of pCO_2 along Tana River Basin. The *center line*, *box extent*, *error bars*, and *dots* denote the 50th, 25th and 75th, 10th and 90th, and outliers of estimates.

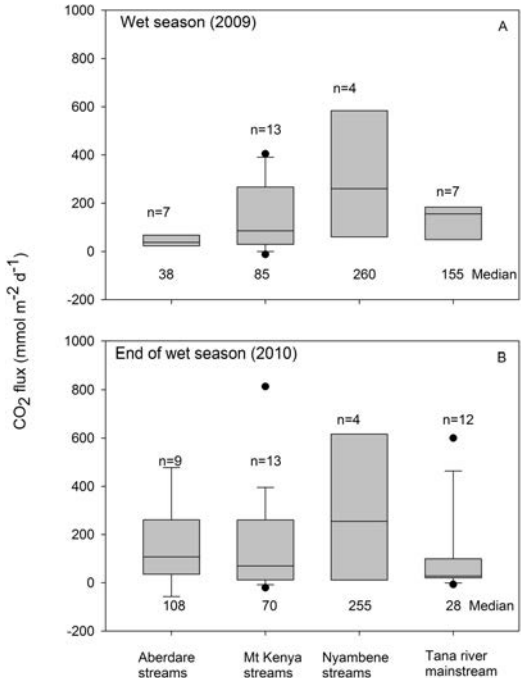

Fig. 7. Boxplots of CO_2 effluxes along Tana River Basin during **(A)** Wet season, **(B)** End of the wet season. The *center line*, *box extent*, *error bars*, and *dots* denote the 50th, 25th and 75th, 10th and 90th, and outliers of estimates.

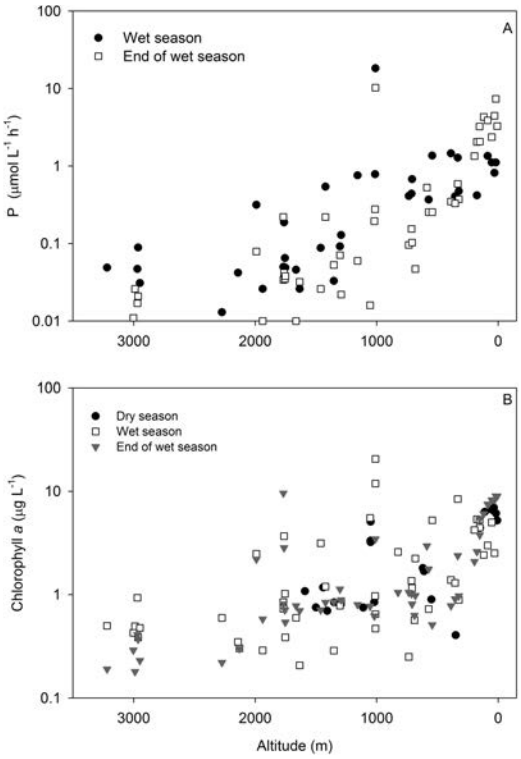

Fig. 8. Altitudinal profile of **(A)** primary production and **(B)** chlorophyll *a* along Tana River Basin during different sampling seasons.

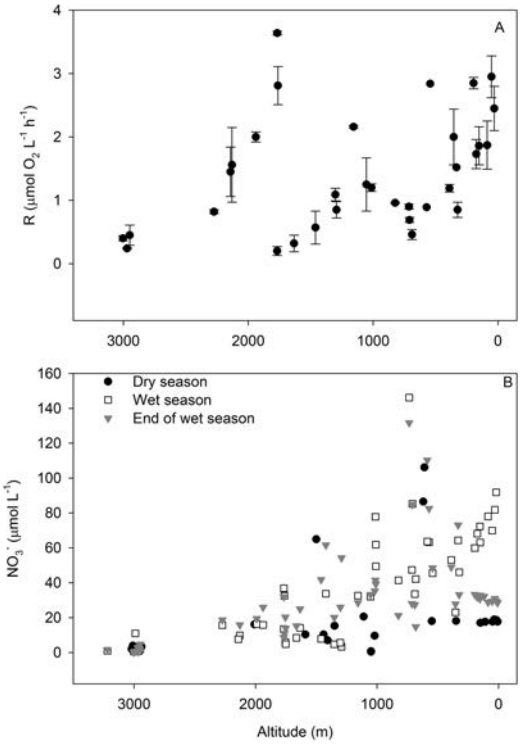

Fig. 9. Altitudinal profile of **(A)** respiration rate during 2009 wet season, and **(B)** nitrate concentrations along Tana River Basin during three sampling seasons.

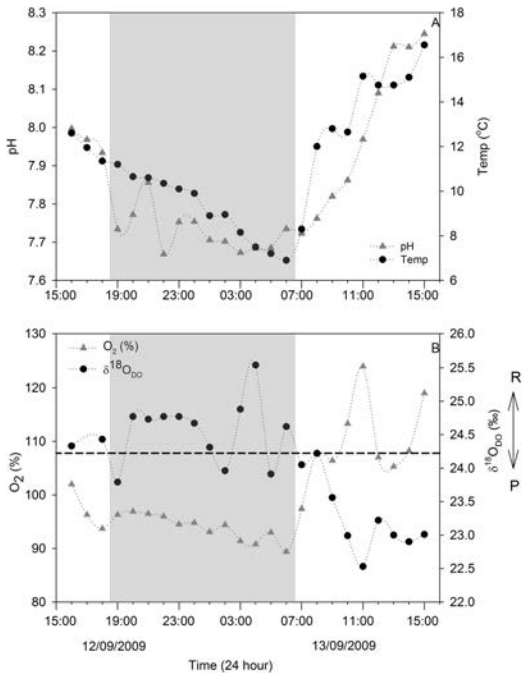

Fig. 10. Diurnal fluctuations of **(A)** pH and temperature and, **(B)** δ^{18}O-DO and % saturation of dissolved oxygen at Chania stream. Night-time is indicated in grey.

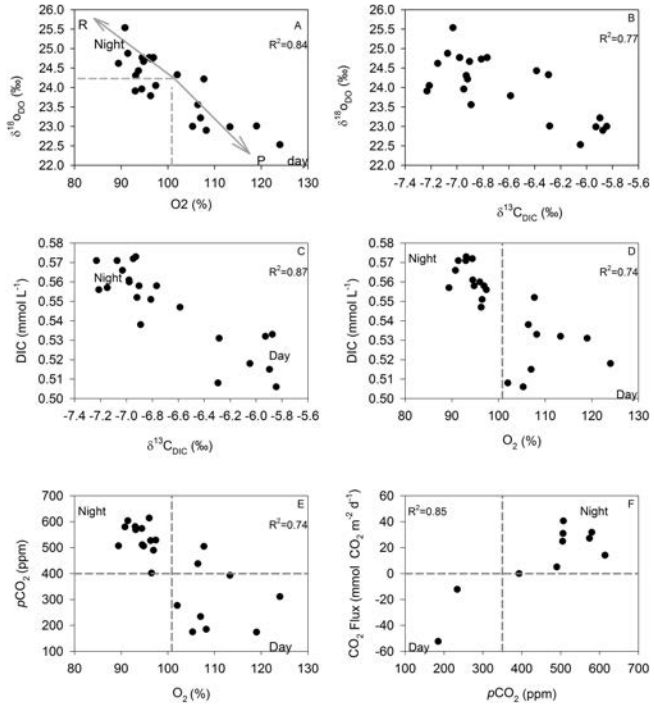

Fig. 11. Cross-plots showing behaviour of different biogeochemical parameters during the diurnal cycle at Chania stream between 12 September 2009 and 13 September 2009.

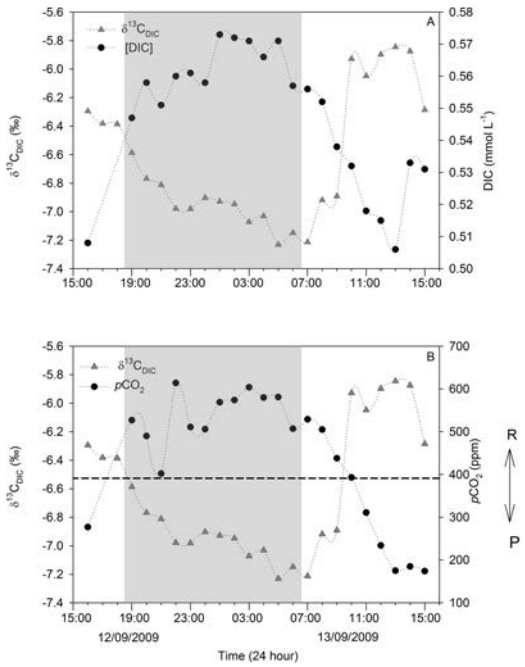

Fig. 12. Diurnal fluctuations of **(A)** $\delta^{13}C_{DIC}$ and DIC concentrations and, **(B)** $\delta^{13}C_{DIC}$ and pCO_2 at Chania stream. Night-time is indicated in grey.

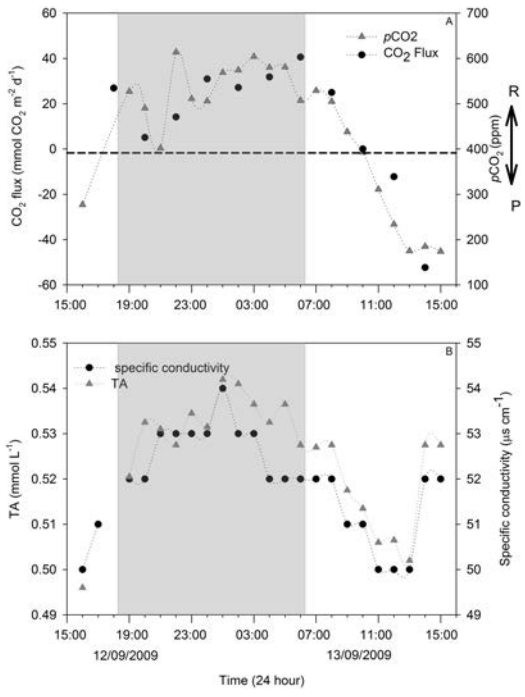

Fig. 13. Diurnal fluctuations of **(A)** CO_2 effluxes and pCO_2 fluxes and **(B)** TA and specific conductivity at Chania stream. Night-time is indicated in grey.

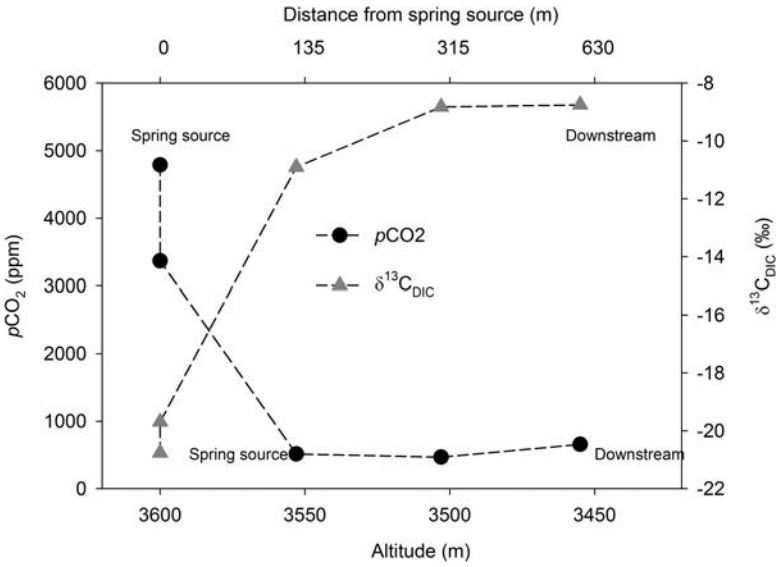

Fig. 14. Cross-plots showing behaviour of pCO_2 fluxes and $\delta^{13}C_{DIC}$ at Satima spring groundwater source in the headwaters of Aberdare Range.